

Detection of a transiting Hot Jupiter around WASP-44

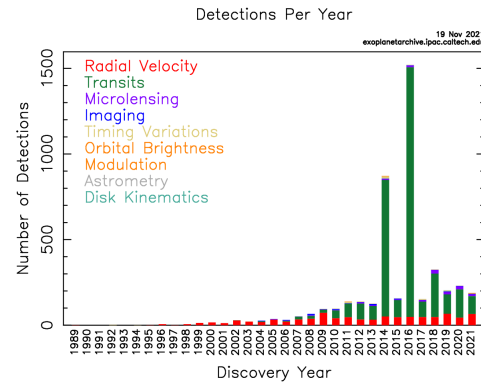
Adriana Barbieri

Alessandro Bianchetti

December 9, 2021

Abstract

In the following report we work on WASP-44 b, an exoplanet orbiting around its G-type mother star, located in the constellation of Cetus. We first take a look at its atmospheric parameters and derive mass and radius (Morton 2015). Then, we correct for limb darkening effect in different ways (Claret et al. 2011, Claret 2017, Claret 2018). We also take some images taken by Copernico at the Asiago Observatory into consideration and, after proper correction, we use them to extract the light curve of the alleged planet.



<https://exoplanetarchive.ipac.caltech.edu/>

In this report we focus on WASP-44 b, a Jupiter-size planet orbiting around a G-type star, located in the constellation of Cetus. Among the numerous available reports on the planet, we decided to make a conservative choice and avoid any result which is not inferred via spectroscopy. This leads us to rule out several papers about the object, and only work with the discovery paper (Anderson et al. 2011). In this paper, estimates of the atmospheric parameters of WASP-44 are provided via an analysis of the width of spectral lines.

1 Introduction

Confirmed exoplanets are growing in number year by year, and transit method is nowadays a widely spread method. Most planets nowadays are discovered by tracing the lightcurve and searching for any sign of a weakening in the flux.

2 Theoretical recap

TODO

- a brief overview of the transit method
- a comment on the bias of the transit method (big planets, close to the star)]

3 Data analysis

3.1 Inferring mass and radius

The H_α line was used to determine the effective temperature (T_{eff}), while the NaI D and MgI b lines were used as surface gravity ($\log g^*$) diagnostics (Anderson et al. 2011). The elemental abundances, including $[Fe/H]$ were determined from equivalent width measurements of several clean and unblended lines. This led to proper estimation of the atmospheric parameter triplet T_{eff} , $\log g^*$ and $[Fe/H]$. Quoted errors include statistical uncertainties only. In the same conservative spirit we previously showed, we add in quadrature a further term to the errors of all three parameters (Sousa et al. 2011). We're in fact more interested in an accurate result rather than a precise one. This leads to the following results

T_{eff} (K)	$\log g^*$	$[Fe/H]$
5400 ± 162	4.5 ± 0.2	0.06 ± 0.11

3.2 Limb darkening correction

Limb darkening is an important effect when observing a star, everything but negligible. In short, the edges of the luminosity profile of a star always look darker: this is because there is a physical, constant distance L at which optical depth is equal to unity, further than which we cannot observe (photons do not reach us). This characteristic size, however, can go deep inside the hot layers of the star if we look straight to the center, being L radial, while it can stop at colder, outer layers if we look at the edges of the star, since L and our LOS are not radial anymore.

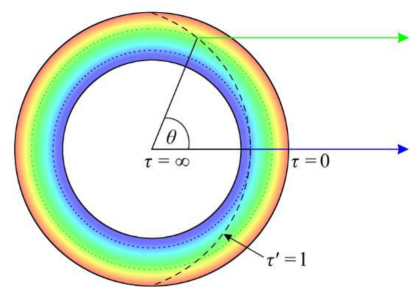


Figure 1: Limb darkening effect scheme. Credits to <https://ediss.sub.uni-hamburg.de>

Correcting for this effect may be challenging. In fact we can measure it directly only for the Sun, while we need to model it somehow for any other star, meaning figure out a proper law for the intensity decrease $I(\mu)$, where $\mu = \sqrt{1 - r^2}$. Many choices are plausible at this point: a uniform behaviour, a linear, a quadratic, a square-root or a logarithmic law are all valid guesses. Parametrizing such laws introduces the so-called *LD-coefficients*, which will depend on the stellar parameters. Knowing the latter relationship (for instance calibrating it based on a large sample of stars) allows to obtain the coefficients directly from the atmospheric parameters. The alternative way is fitting the light curve leaving the coefficients free.

The choice of the functional dependence on μ is a delicate one. Multiple approaches can be followed, basing on different papers. This analysis is tackled in A.

3.3 Bias and flat field correction

CCD (Charged Coupled Device) are the privileged detectors for photon counting, thanks to their great quantum efficiency. The images produced are *raw* and must be properly *pre-reduced* before being analysed. Pre-reduction goes through different steps:

- **bias** is the individual pixel-to-pixel offset level, and it's a zero-exposure instrumen-

tal factor, thus it's always an added contribution to any signal. Therefore it must be removed to isolate the photons of astrophysical origin. The root mean square of the bias corresponds to the so-called *readout noise*. We perform an average out across all the pixels to get an estimate of the bias;

- a **flat field** is a calibration image obtained by illuminating homogeneously the pupil of the telescope, using twilight sky or appropriate, back-lighted screens. This correction factor is to be applied on each pixel and then also normalised, after the overall bias correction;
- **differential photometry** is a great way to keep track of any noise variation. The idea is to take a reference star close enough to the target: any environmental or instrumental variation will affect both sources. Working with flux ratios will make only astrophysical variations evident!

For pre-reductions steps, we use the code *huggy*. We first perform bias correction, than the flat field correction. The corrected images are ready for aperture synthesis.

3.3.1 Bias correction

We run *huggy-bias.e* inputting the raw images.

```
huggy-bias.e A*.fits
```

Many bias images are produced, displaying the zero offset of the pixel board. *Master bias* is the average of all these files. Plotting the intensities of offset level of the pixels yields a concrete view of the correction.

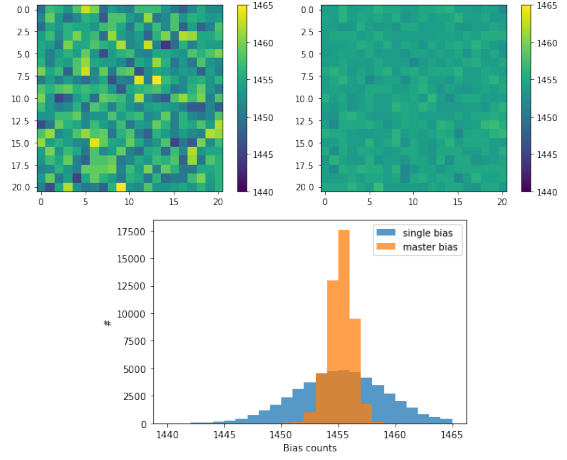


Figure 2: Comparison between random bias frame and master bias

Note that the master bias frame distribution is peaked and much closer to a unique constant value, as all pixels behaved in the same way, like in an ideal situation. We can see this even numerically, by looking at the dispersions of the above distributions: $\sigma_{rb} = 3.82$ and $\sigma_{mb} = 0.89$.

3.3.2 Flat field correction

We now run *huggy-flat.e* inputting a normalization fraction, meaning the fraction of pixels we want to account for, ruling out the sides which are often polluted by overscan columns. These are visible in the form of dark stripes on the sides of any flat field take. Then we have to input the overscan values, usually set to 0. After, that we need to provide the master bias file, which will be subtracted from the data. Finally, we input all the flat fields available.

```
huggy-flat.e 0.9 0 0 mb.fits A*.fits
```

This will produce an output file showing the average response of pixels to an external light source. Minor differences in such response are important and must be accounted for.

3.4 Final correction

The final step is applying the correction files obtained in the previous parts.

```
huggy-correct.e mb.fits mfn.fits A*.fits
```

The final correction code requires the master bias and the normalised master flat, and of course all the target images, that are going to be all corrected.

3.5 Extracting the light curve

We are approaching the very heart of this analysis, preparing for aperture synthesis. We now need to display the science images, make sure to identify the correct target and select a proper background analysis around it. To do that, we have to properly circle the source and create a slightly larger circle around it (*ds9* was the used tool). The same procedure must be repeated (with the same inner and outer radii) on a properly selected reference star, close to and roughly as bright as the target. We hereby report the coordinates of the target and of the chosen reference star, in pixel units.

	x_c	y_c
Target	170	37
Reference	288	57

$$R_{in} = 11, R_{out} = 20$$

Now we need to call *huggy-psf.e* and input the coordinates of the center of the target, the inner and outer radii, and a random corrected image.

```
huggy-psf.e x0 y0 Rin Rout A*.fits
```

This yields information about the Point Spread Function, meaning how the the flux is distributed as a function of the distance from the core of the source. The ouput displays the radii at which we find 90, 95 and 99% of the total flux. We tale note of this output.

Photometry analysis is carried out by *sentinel.e*, which needs the coordinates of the target and of the reference stars, followed by the radii of two selected apertures from the previous output. Also, we need again inner and outer radii of the selected region for the analysis, as well as the full-corrected images of the target.

```
sentinel.e x0 y0 xr yr a1 a2 Rin Rout c  
A*.corr.fits
```

where $c = \{1, 2\}$ selects the centroiding method (gaussian/moment). For a relatively faint star like ours ($J \approx 11$) our choices are $a_1 = 4.71$ and $a_2 = 5.97$, corresponding to 90 and 95%. The *sentinel* output is the starting point for TASTE analysis.

4 Conclusions

A Limb darkening analysis

A.1 Claret 2017

We can represent data tables in Claret 2017 as 2D histograms, after proper unfolding of the data tables attached to the paper. To do that, we first fix metallicity, then gravity and see how the corresponding LD coefficients c_1 and c_2 depend on all three atmospheric parameters.

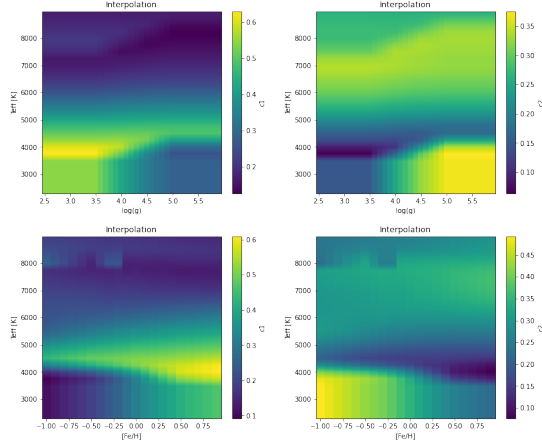


Figure 3: LD coefficient with fixed metallicity, fixed gravity

Furthermore, it's very interesting to check the strength of the dependance on each atmospheric parameters. Turns out LD coefficients are essentially a function of temperature, and minor dependences on gravity and metallicity can be barely appreciated.

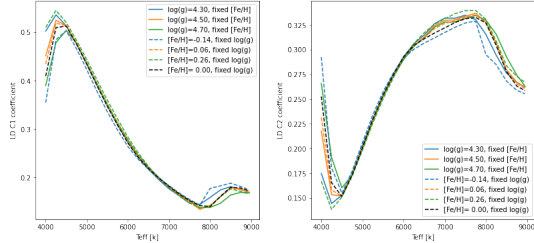


Figure 4: LD coefficient as a function of atmospheric parameters

A relevant dependance on gravity and metallicity can only be noticed at high temperatures, where we should carefully select the proper curve. But in the range we're interested in ($\approx 5400K$) the curve is degenerate and the choice of these parameters is secondary.

We perform a Montecarlo simulation, generating 1000 random atmospheric parameters around the actual ones. Even in this case we see that the distribution of the fixed-metallicity estimates is almost overlapping with the fixed-

gravity one, thus confirming c_1 and c_2 not very sensitive on metallicity and gravity.

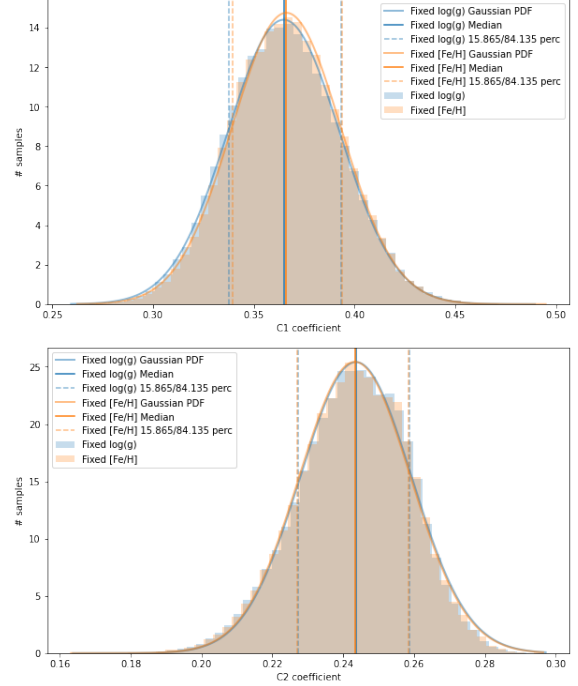


Figure 5: Montecarlo simulation for c_1 and c_2 , for fixed metallicity and for fixed gravity

The two estimates are well compatible, thus authorizing a weighted average: $c_1 = 0.366 \pm 0.019$ and $c_2 = 0.243 \pm 0.011$.

Another way to deal with the same table is by selecting from the set the two closest stars to ours, instead of just one. The rest of the procedure is the same as just explained, leading to other estimate of the LD coefficients.

A.2 Claret 2018

Only the zero metallicity case is now considered.

B Time correction

References

- Morton, Timothy D. (2015). eprint: 1503.010
Claret, A. et al. (2011). *A&A* **529**, A75
Claret, A. (2017). *A&A* **600**, A30
Claret, A. (2018). *A&A* **618**, A20
Anderson, D.R. et al. (2011). *MNRAS* **422**
Sousa, S.G. et al. (2011). *A&A* **533**, A141